

AD-A242 742

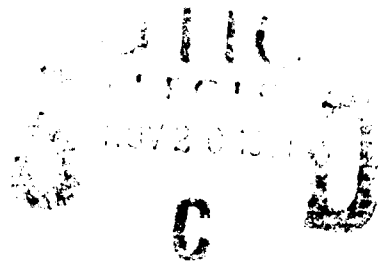


van  
②



US ARMY  
LABORATORY COMMAND  
MATERIALS TECHNOLOGY LABORATORY

AD



MTL TR 91-37

# METAL INJECTION MOLDING OF TUNGSTEN HEAVY ALLOYS: SBIR PHASE I

October 1991

GARY M. ALLEN  
Technology Associates Corporation  
17911 Sampson Lane  
Huntington Beach, CA 92647

FINAL REPORT

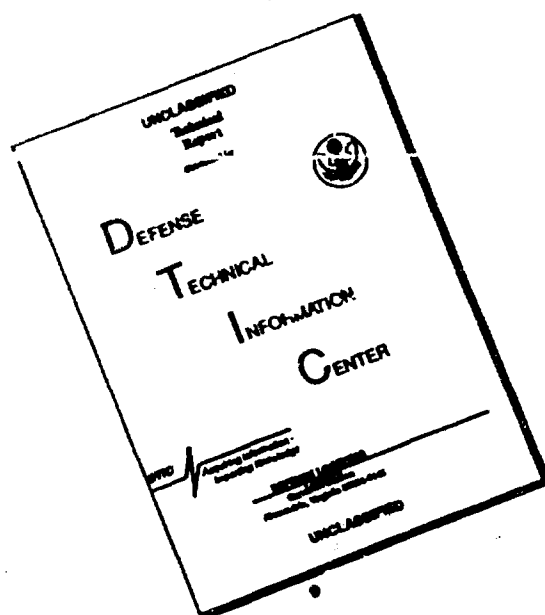
Contract DAAL04-90-C-0018

Approved for public release; distribution unlimited.

Prepared for

U.S. ARMY MATERIALS TECHNOLOGY LABORATORY  
Watertown, Massachusetts 02172-0001

# DISCLAIMER NOTICE



THIS DOCUMENT IS BEST QUALITY AVAILABLE. THE COPY FURNISHED TO DTIC CONTAINED A SIGNIFICANT NUMBER OF PAGES WHICH DO NOT REPRODUCE LEGIBLY.

The findings in this report are not to be construed as an official Department of the Army position, unless so designated by other authorized documents.

Mention of any trade names or manufacturers in this report shall not be construed as advertising nor as an official indorsement or approval of such products or companies by the United States Government.

#### DISPOSITION INSTRUCTIONS

Destroy this report when it is no longer needed.  
Do not return it to the originator.



Block No. 20

ABSTRACT

The objective of SBIR A90-133 is to investigate the feasibility of injection molding tungsten heavy alloys into net or near-net shape parts. The focus of Phase I was to demonstrate (on a laboratory scale) that powder injection molding (PIM) can provide parts with equivalent or superior sintered material properties to those that have been achieved for press/sintering heavy alloys of similar compositions. In addition, geometric shrinkage(s) and key process variables were identified and analyzed.

TABLE OF CONTENTS

List of Figures . . . . . ii

Objective . . . . . 1

Experimental Procedure . . . . . 1

Conclusion . . . . . 3

Results and Discussion . . . . . 4

    Elemental Powder Analysis . . . . . 4

    Powder Blending . . . . . 7

    Solid Loading Curve . . . . . 8

    Feedstock Rheology . . . . . 9

    Feedstock Mixing . . . . . 12

    Prototype Test Mold . . . . . 12

    Injection Molding . . . . . 14

    Debinding (Solvent) . . . . . 14

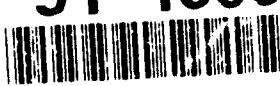
    Furnacing (Thermal Debinding and Sintering) . . . . . 15

    Part Dimensioning . . . . . 17

    Material Property Testing . . . . . 17

    Chemical Analysis . . . . . 25

Accession For  
NILES UKA&I ✓  
7743 Tab  
Approved  
Justification  
By \_\_\_\_\_  
Distribution  
Availability Code  
Date \_\_\_\_\_  
A-1

91-16056  


91 1120 044

## LIST OF FIGURES

Figure 1.	Malvern Elemental Powder Particle Size Distributions. . . . .	5
Figure 2.	Malvern Alloy Particle Size Distribution. . . . .	6
Figure 3.	H.L. Feedstock Rheological Stress/Strain Curves . . . . .	10
Figure 4.	L.L. Feedstock Rheological Stress/Strain Curves . . . . .	.11
Figure 5.	Illustration of Tensile Test Bar Specimen . . . . .	.13
Figure 6.	Test Bar Shrinkages . . . . .	.16
Figure 7.	Test Bar Densities. . . . .	.18
Figure 8.	Test Bar Microhardness Data. . . . .	.19
Figure 9.	Test Bar Tensile Properties . . . . .	.20
Figure 10A.	Microstructure SEM Photomicrographs (0.4 Volume Fraction of Solid) . . . . .	.22
Figure 10B.	Microstructure SEM Photomicrographs (0.5 Volume Fraction of Solid) . . . . .	.23
Figure 11.	Tungsten Grain Characteristics . . . . .	.24
Figure 12A.	Matrix Chemistry - EDS Analysis (0.4 Volume Fraction of Solid) . . . . .	.26
Figure 12B.	Matrix Chemistry - EDS Analysis (0.5 Volume Fraction of Solid) . . . . .	.27
Figure 13.	Tungsten Grain Alloy Chemistry . . . . .	.28
Figure 14.	Matrix Chemistry - Quantitative Analysis . . . . .	.29
Figure 15.	Carbon/Oxygen Acquisition During PIM Processing . . . . .	.30

## SBIR A90-133 FINAL REPORT

### Metal Injection Molding of Tungsten Heavy Alloys

#### OBJECTIVE

The objective of **SBIR A90-133** is to investigate the feasibility of injection molding tungsten heavy alloys into net or near-net shape parts. The focus of **Phase I** was to demonstrate (on a laboratory scale) that **powder injection molding (PIM)** can provide parts with equivalent or superior sintered material properties to those that have been achieved for press/sintering heavy alloys of similar compositions. In addition, geometric shrinkage(s) and key process variables were identified and analyzed.

#### EXPERIMENTAL PROCEDURE

A sample test geometric shape was identified and a (injection molding) tool was constructed to prototype green parts. **Two feedstock formulations** with different volume fraction solid loadings were specified as test parameters. Test specimens were then debound, sintered, heat treated and tested for resultant material properties and alloy chemistry. This investigation was divided into **twelve tasks** that are identified in the following listing.

##### Task 1: Elemental Particle Analysis

All elemental particles were analyzed using **laser diffraction** analysis sizing hardware/software incorporated in a Malvern Master Sizer. They were also examined using an optical microscope.

##### Task 2: Powder Blending

Elemental W, Ni and Fe powders were **mechanically blended** in a V-blender to form a master alloy.

##### Task 3: Solid Loading Curve

The solid loading curve was constructed after adding small powder increments to the feedstock mixer which established the loading limits (dictated by the equipment) between 0.4 and 0.5. These were established as the two test sample loadings used in this investigation.



**Task 4: Feedstock Rheology**

Feedstock viscosity characteristics were established by the rheological profiles for both sample feedstock lots.

**Task 5: Feedstock Mixing**

Prototype feedstock was mixed in a Scott Turbon Mixer utilizing the master powder alloy and a three part thermoplastic/lubricant binder formulation.

**Task 6: Prototype Test Mold**

The prototype test specimen mold was produced and dimensionally modified by Diversified Mold, Inc. (Huntington Beach, CA).

**Task 7: Injection Molding**

Injection Molding was performed in a Arburg (Model 305-211-700) with test specimens provided for both solid loading volume fractions.

**Task 8: Debinding (Chemical)**

The green test specimens were chemically debound with 1-1-1 trichloroethane and thermally dried in a Bowden Liquid Turbo Charged system.

**Task 9: Furnacing (Thermal Debinding and Sintering)**

The parts were thermally debound, sintered and heat treated using furnacing cycles that sequentially interfaced atmospheres of dry and wet hydrogen, and vacuum.

**Task 10: Part Dimensioning**

The sintered parts were measured for width, length and thickness dimensions; and the shrinkage percentages were calculated.

**Task 11: Material Property Testing**

The resultant material properties for each volume fraction solid loading were established by obtaining the following parameters for each sintered sample set:

Density  
Hardness  
Microhardness  
Tensile Properties  
Matrix Volume Fractions  
Grain Size

#### Task 12: Chemical Analysis

The alloy chemistry of the blended powder and the sintered samples were compared for **carbon content**. The **alloy chemistry** of both sintered sample lots was evaluated by Energy Dispersive Spectroscopic (EDS) analysis.

#### CONCLUSION

PIM is a **viable process** for producing **tungsten heavy alloys** since the resultant properties were comparable to press/sintered alloys having similar compositions. The **processing conditions** within PIM did not produce any significant changes in sintered density, hardness, microhardness, and the matrix alloy chemistry between samples. The **shrinkages** were different for the two volume fractions of solid loading, but the variation in the shrinkages for each set was within 1%. Chemical debinding when combined with the thermal debinding resulted in total binder removal in all samples without any **residual carbon**. The sintered densities, mechanical properties, and the microstructures were all similar to normal press/sintered alloys.

In conclusion, **Phase I** demonstrated that **PIM** can achieve production of near net shaped tungsten heavy alloys parts that result in little or no machining. Recent developments in alloying conventional tungsten heavy alloys suggest the feasibility of fabricating high strength, high hardness, near net shaped parts for numerous applications. The success of **Phase I**, provides a **strong base** for further research to develop military and commercial products based on tungsten heavy alloys.

## RESULTS AND DISCUSSION

### Elemental Powder Analysis

Technology Associates Corporation ("TAC") ordered elemental powders from the following sources:

W Powder	GTE Products Corporation Towanda, PA 18848
Fe Powder	GAF Chemical Corporation Linden, NJ 07036
Ni Powder	Nova Met Specialty Products Corporation Wyckoff, NJ 07481

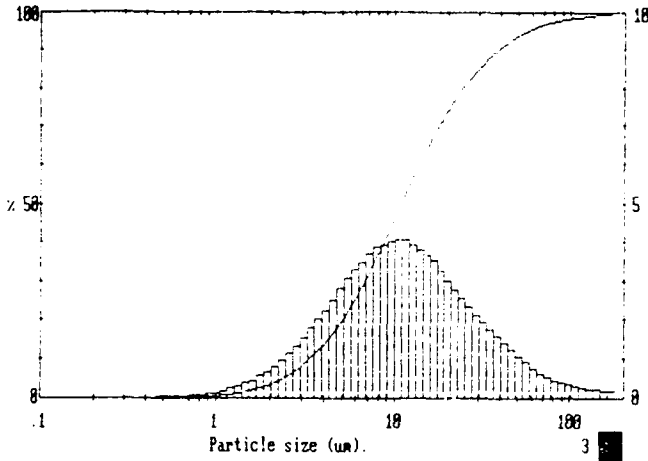
They were processed to determine particle size distributions. This was accomplished with a Malvern Master Sizer.

The results are summarized graphically and numerically in Figure 1. The following table lists the summary statistics taken from the histograms and cumulative distributions:

<u>Powder</u>	<u>Mean (<math>\mu\text{m}</math>)</u>	<u>Std Dev. (<math>\mu\text{m}</math>)</u>
W	10.82	9.50
Ni	10.28*	8.79
Fe	6.52	7.32
Alloy	12.43	9.99

\* Takes into account a small portion of agglomerated iron particles due to the limited range of ultrasonic interface as illustrated in Figure 1 (lowest graph).

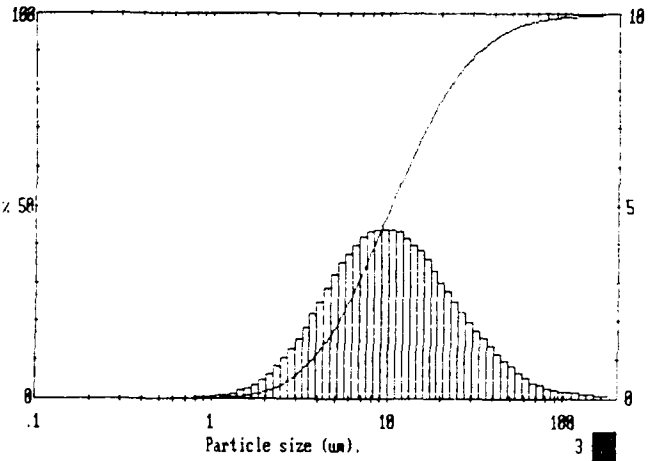
Figure 2 illustrates the interactive nature of the Fe powder in forming the master alloy.



SAMPLE DETAILS: TUNGSTEN

High Size	In %	High Size	In %	High Size	In %	High Size	In %	High Size	In %	High Size	In %	Span
150	0.2	14.4	0.5	23.0	0.8	18.25	3.9	2.95	1.3	1.06	0.1	D(4.2)
164	0.2	58.7	1.7	21.0	0.9	17.51	4.2	2.69	1.0	0.96	0.0	15.65um
149	0.2	53.4	1.1	19.1	0.3	16.84	3.5	2.45	0.6	0.88	0.0	D(3.2)
136	0.2	48.7	1.2	17.4	0.5	16.23	3.3	2.33	0.6	0.80	0.0	4.92um
124	0.2	44.3	1.4	15.9	0.7	15.67	3.1	2.23	0.5	0.73	0.0	3.57um
113	0.2	40.4	1.6	14.4	0.8	15.17	3.0	2.185	0.4	0.66	0.0	D(2.5)
103	0.2	36.8	1.8	13.2	1.0	14.71	2.9	2.168	0.3	0.60	0.0	32.4um
93.6	0.4	33.5	2.0	12.0	1.1	14.29	2.8	2.153	0.2	0.55	0.0	D(1.5)
85.2	0.4	30.5	2.1	10.9	1.1	13.91	2.7	2.140	0.1	0.50	0.0	D(0.1)
77.6	0.6	27.8	2.3	9.94	1.1	13.56	2.6	2.127	0.1	0.47	0.0	D(0.1)
70.7	0.6	25.3	2.6	9.05	1.1	13.24	2.5	2.116	0.1	0.44	0.0	D(0.1)

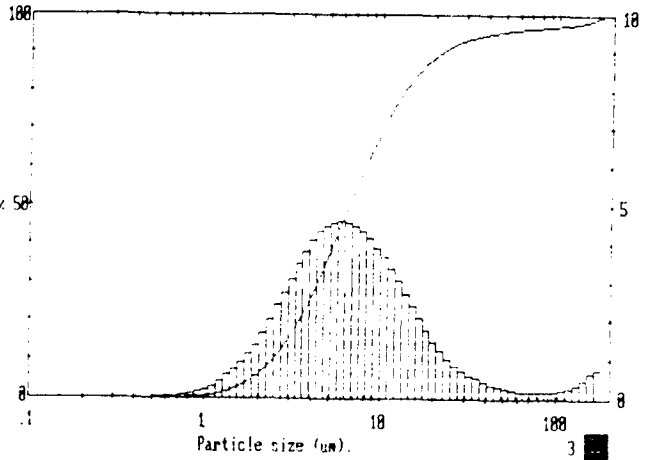
Source = :Sample Beam length = 2.2 mm Model indep  
 Residual = 0.411 %  
 Focal length = 100 mm Observation = 0.2562 Volume Conc. = 0.0855%  
 Presentation = 0010 Volume distribution Sp.S.R 0.8522 #/cc



SAMPLE DETAILS: NICKEL

High Size	In %	High Size	In %	High Size	In %	High Size	In %	High Size	In %	High Size	In %	Span
180	0.1	64.4	0.5	23.0	0.8	18.25	4.3	2.95	1.3	1.06	0.1	D(4.2)
164	0.1	58.7	0.7	21.0	0.9	17.51	4.2	2.69	1.0	0.96	0.0	15.65um
149	0.1	53.4	0.8	19.1	0.3	16.84	4.0	2.45	0.6	0.88	0.0	D(3.2)
136	0.1	48.7	1.0	17.4	0.5	16.23	3.8	2.33	0.6	0.80	0.0	4.92um
124	0.2	44.3	1.2	15.9	0.8	15.67	3.5	2.23	0.5	0.73	0.0	3.57um
113	0.2	40.4	1.4	14.4	1.0	15.17	3.2	2.185	0.4	0.66	0.0	D(2.5)
103	0.2	36.8	1.6	13.2	1.2	14.71	2.9	2.168	0.3	0.60	0.0	32.4um
93.6	0.2	33.5	1.8	12.0	1.3	14.29	2.8	2.153	0.2	0.55	0.0	D(1.5)
85.2	0.3	30.5	2.0	10.9	1.4	13.91	2.7	2.140	0.1	0.50	0.0	D(0.1)
77.6	0.3	27.8	2.1	9.94	1.4	13.56	2.6	2.127	0.1	0.47	0.0	D(0.1)
70.7	0.4	25.3	2.2	9.05	1.4	13.24	2.5	2.116	0.1	0.44	0.0	D(0.1)

Source = :Sample Beam length = 2.2 mm Model indep  
 Residual = 0.356 %  
 Focal length = 100 mm Observation = 0.2188 Volume Conc. = 0.0235%  
 Presentation = 0010 Volume distribution Sp.S.R 0.7931 #/cc

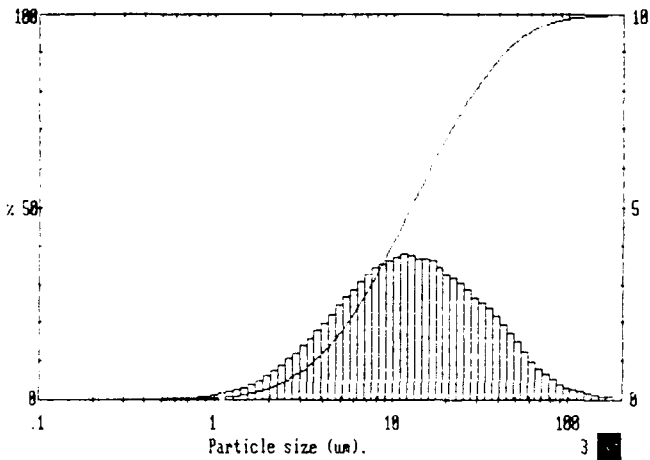


SAMPLE DETAILS: 100%

High Size	Under %	High Size	Under %	High Size	Under %	High Size	Under %	High Size	Under %	High Size	Under %	Span
180	100	64.4	99.5	23.0	99.2	18.25	98.1	2.95	95.8	1.06	95.6	D(4.2)
164	99.8	58.7	99.2	21.0	98.9	17.51	98.0	2.69	97.0	0.96	96.9	15.65um
149	99.7	53.4	98.9	19.1	98.7	16.84	98.5	2.45	97.9	0.88	97.8	D(3.2)
136	99.6	48.7	98.7	17.4	98.5	16.23	98.3	2.33	98.0	0.80	97.9	4.92um
124	99.5	44.3	98.5	15.9	98.3	15.67	98.1	2.23	97.9	0.73	97.8	3.57um
113	99.4	40.4	98.3	14.4	98.1	15.17	97.9	2.185	97.8	0.66	97.7	D(2.5)
103	99.3	36.8	98.1	13.2	97.9	14.71	97.7	2.168	97.7	0.60	97.6	32.4um
93.6	99.2	33.5	97.9	12.0	97.7	14.29	97.6	2.153	97.6	0.55	97.5	D(1.5)
85.2	99.1	30.5	97.7	10.9	97.5	13.91	97.5	2.140	97.5	0.50	97.4	D(0.1)
77.6	99.0	27.8	97.5	9.94	97.4	13.56	97.4	2.127	97.4	0.47	97.3	D(0.1)
70.7	98.9	25.3	97.3	9.05	97.3	13.24	97.3	2.116	97.3	0.44	97.2	D(0.1)

Source = :Sample Beam length = 2.2 mm Model indep  
 Residual = 0.154 %  
 Focal length = 100 mm Observation = 0.2417 Volume Conc. = 0.0181%  
 Presentation = 0010 Volume distribution Sp.S.R 1.1124 #/cc

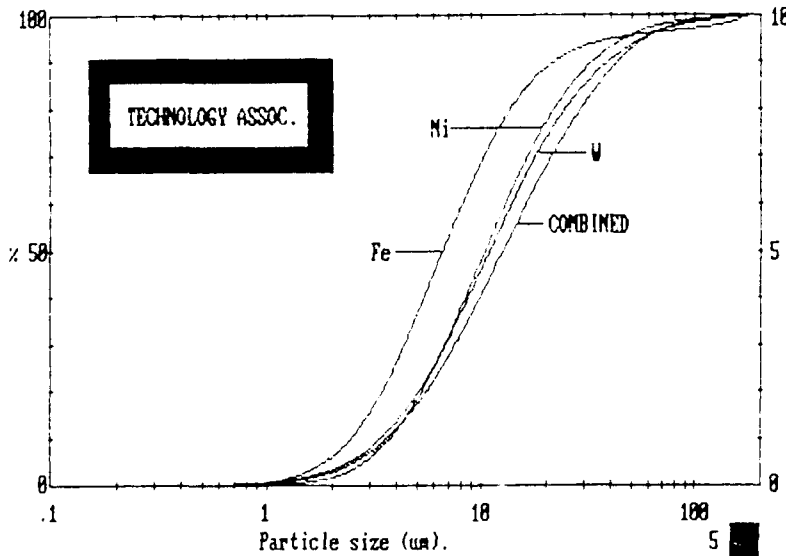
Figure 1. Malvern Elemental Powder Particle Size Distributions.



SAMPLE DETAILS: IRON-NICKEL-TUNGSTEN COMBINED

High Size	In %	High Size	In %	High Size	In %	High Size	In %	High Size	In %	High Size	In %	Span
180	0.1	164.4	1.0	123.0	3.2	10.25	1.4	2.95	1.2	1.46	0.1	D(4,3)
164	0.1	58.7	1.2	21.0	3.3	17.51	3.3	2.69	1.1	10.96	0.1	19.17um
149	0.1	53.4	1.5	19.1	3.5	16.84	3.1	2.45	0.9	10.88	0.1	
136	0.2	48.7	1.7	17.4	3.6	16.23	2.9	2.23	0.7	10.80	0.1	D(1,3)
124	0.2	44.3	1.9	15.9	3.7	15.67	2.7	2.03	0.6	10.73	0.0	7.75um
113	0.3	40.4	2.2	14.4	3.7	15.17	2.5	1.85	0.5	10.66	0.0	
103	0.3	36.8	2.5	13.2	3.7	14.71	2.2	1.65	0.4	10.60	0.0	D(0.5,1)
93.6	0.4	32.5	2.8	12.0	3.8	14.29	2.0	1.53	0.3	10.55	0.0	4.55um
85.2	0.5	30.5	3.0	10.9	3.7	13.91	1.8	1.40	0.3	10.50	0.0	
77.6	0.7	27.8	3.3	9.94	3.6	13.56	1.6	1.3	0.2			D(0.1,1)
70.7	0.8	25.3	3.1	9.05	3.5	13.24	1.4	1.1	0.2			3.58um

Source = :Sample Beam length = 2.2 mm Model indep  
 Focal length = 100 mm Residual = 0.506 %  
 Presentation = 001% Volume distribution Sp.S.R. 0.7746 #/cc



7001 0010 1m10072m  
 SAMPLE DETAILS: IRON-NICKEL-TUNGSTEN COMBINED

Figure 2. Malvern Alloy Particle Size Distribution.

### Powder Blending

The elemental W, Ni, and Fe were **processed** in a roller mill and then **blended** for five hours in a V-blender to the following ratios:

<u>Metal</u>	<u>Weight (gm)</u>	<u>Weight Percentage(%)</u>	<u>Density(g/cc)</u>
W	19,000	95.0	19.30
Ni	800	4.0	8.90
Fe	200	1.0	7.87

The powders were studied using an optical microscope which displayed the great affinity of Fe particles for any other elemental powder upon contact. This resulted in powder agglomerates in the final alloy which was confirmed by the cumulative powder size distribution shown in Figure 2.

## Solid Loading Curve

The metal powder master alloy was mixed with the TAC polymer binder in a **double planetary** Scott Turbon mixer, which had an oil jacket for heating the mixer basket. The solid composition was adjusted to provide a final heavy alloy composition of **95W-4Ni-1Fe** by weight. The binder was first liquified in the double planetary mixer and the elemental powder mixture was added gradually to the molten binder. The initial amount of solid addition was adjusted to yield a 0.3 volume fraction of solid loading. The mixing was continued at a temperature of 177° C (350°F) for 45 minutes after which small samples were taken out from three different areas of the molten feedstock. The density of these samples were carefully measured by water immersion technique. The **solid loading** was increased in small steps to afford different volume fractions in the feedstock. After each increment, the material was mixed before repeating the sample extraction and density measurement. A 0.5 volume fraction of solid loading was selected as a limit as result of mixer mechanical limitations.

The volume fraction of solid loading was calculated from the amounts of binder and solid used in the mixing process. The measured densities for all volume fractions are somewhat lower than the calculated densities. This could be expected as the mixing was accomplished in air. The viscous liquid mass often entraps air within its body and forms minute air bubbles. As the feedstock is cooled, viscosity of the mixture increases very rapidly and the air bubbles are permanently entrapped in the feedstock mixture. Longer mixing times or maintaining a **vacuum** could alleviate this problem. Utilizing a roughing pump vacuum during the mixing step is perhaps the best solution to this problem as it can then bias the diffusivity of the air away from the feedstock mixture.

One of the feedstocks contained **0.5 volume fraction** of solid. Since the viscosity of this mixture was felt to be quite high, it was decided to use a second feedstock with lower volume fraction of solid adjusted to 0.4. The point where the solid-binder mixture was no longer a viscous fluid and mixing became difficult was at 0.5. This was considered to be the **Critical Volume Fraction (CVF)** of solid loading. For subsequent investigations both feedstock loadings were tested.

## Feedstock Rheology

The change in feedstock viscosity with increasing volume fraction of solid is a leading indicator of the CSL since viscosity relates the feedstock shear stress to the shear strain rate. A PIM feedstock that exhibits a visco-elastic nature and a high viscosity will make the molding process difficult. A capillary rheometer provides an excellent method for characterizing the PIM feedstock and was completed on the Rheometrics RDA2. There were two feedstock samples:

Heavy Loading (H.L.): 0.5 volume fraction solid.

Light Loading (L.L.): 0.4 volume fraction solid.

Both feedstock samples were broken, then ground, and finally compressed into 25 mm disks using disposable, serrated and parallel plates.

Both samples were tested in strain sweeps at 10 radians per second at 177°C (350°F) from 0.1% to 100% strain. The samples were also tested in frequency sweeps at 50% strain at 177°C (350°F) from 0.1 to 100 radians/second.

The results of these strain sweeps are plotted in Figures 3 and 4. The notation for each curve can be summarized as follows:

<u>Symbol - Notation</u>	<u>Meaning</u>	<u>Units</u>
G' (◇) - Upper Curve	Heat Dissipation per % Strain	DYN/cm <sup>2</sup>
G'' (Δ) - Middle Curve	Elasticity per % Strain	DYN/cm <sup>2</sup>
η* (˘) - Lower Curve	Viscosity per % Strain	Poise

The H.L. sample showed greater elasticity and structure throughout the test than the L.L. sample. Neither sample showed a linear visco-elastic region down to 0.1% strain. The H.L. sample became more viscous than elastic at 15% strain (Figure 3) while the L.L. sample at 8% strain (Figure 4). The H.L. sample also showed a higher viscosity and viscous modulus throughout the sweep. Finally, the H.L. sample was more strain dependent than the other sample; and thus, it may have been less stable.

The frequency sweeps were done at high strains to simulate processing. The H.L. sample showed higher viscosity at low frequencies for good melt strength, and lower viscosity at high frequencies for easier processing (more shear thinning). The L.L. sample showed less particle associations at higher frequencies. Both samples showed strong associated particles at very low strains. From the data it appeared that the H.L. sample might be easier to process but exhibit a less stable dispersion.



sbir heavy strain sweep 177c

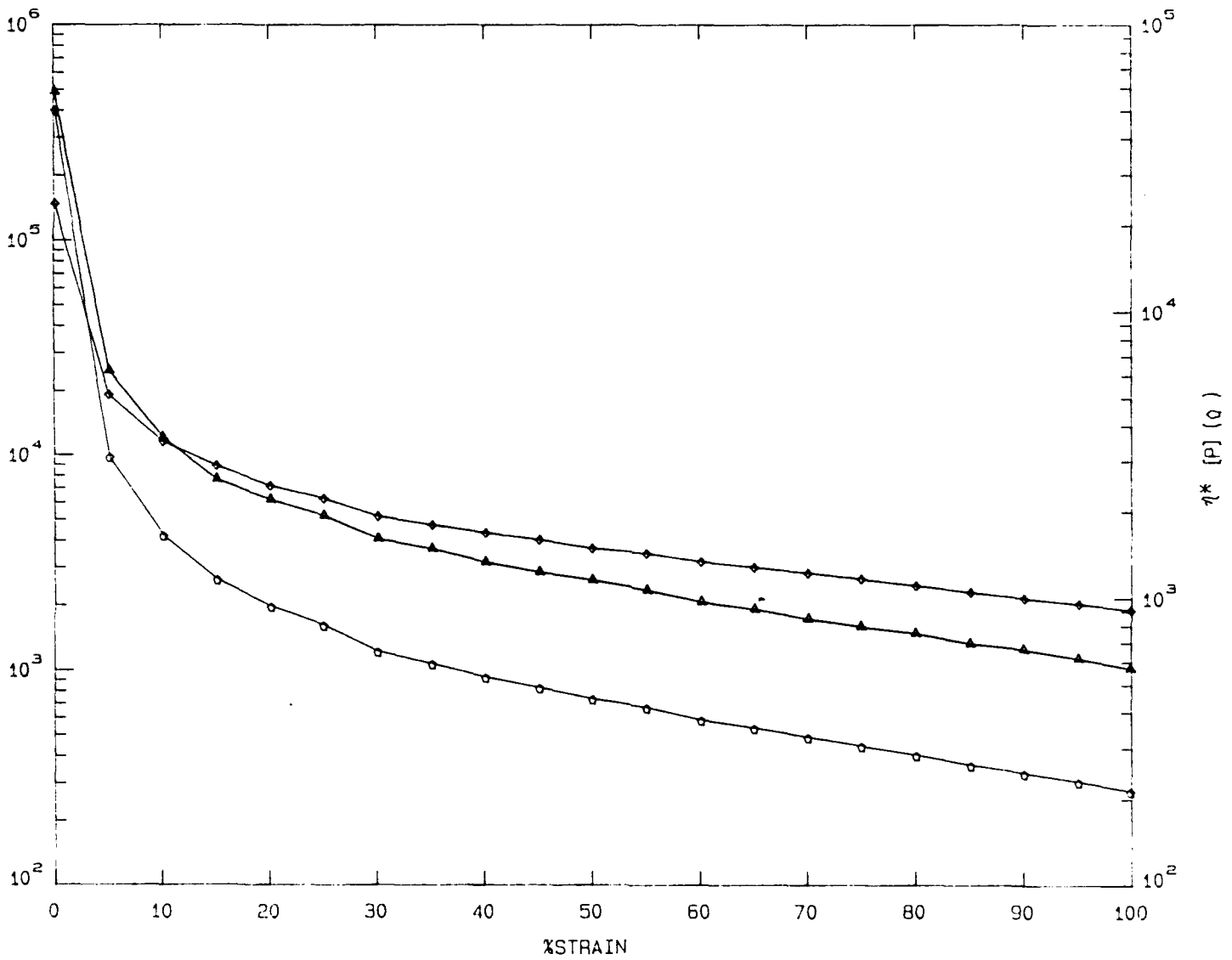


Figure 3. H.L. Feedstock Rheological Stress/Strain Curves at 350° F (177° C).

sbir #1 177c strain sweep light loading

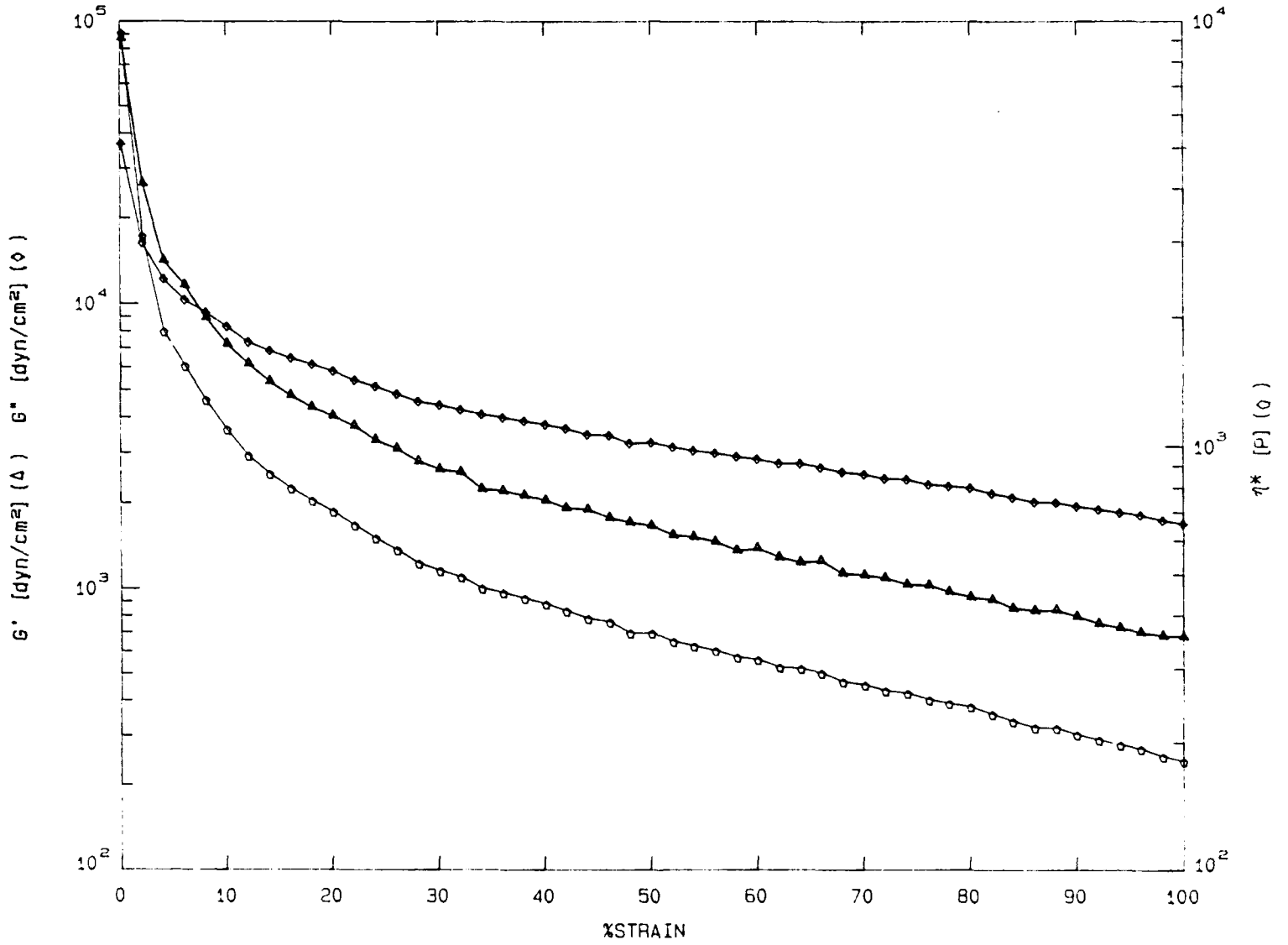


Figure 4. L.L. Feedstock Rheological Stress/Strain Curves at 350° F (177° C).

### Feedstock Mixing

The master powder alloy and the binder matrix were mixed in an oil jacketed, Scott Turbon Double Planetary Mixer. The feedstock formulation was as follows:

<u>0.50 Volume Fraction Solid</u>	<u>Wt. (gm)</u>
W-Ni-Fe (18.18 gm/cc)	5,000.0
Polyethylene (HDPE) (.905 gm/cc)	67.2
Polyalphamethyl Styrene (1.075 gm/cc)	100.8
Lubricant (.913 gm/cc)	<u>168.0</u>
TOTAL	<u>5,336.0</u>

<u>0.40 Volume Fraction Solid</u>	<u>Wt. (gm)</u>
W-Ni-Fe (18.18 gm/cc)	4,440.0
Polyethylene (HDPE) (.905 gm/cc)	112.0
Polyalphamethyl Styrene (1.075 gm/cc)	168.0
Lubricant (.913 gm/cc)	<u>280.0</u>
TOTAL	<u>5,000.0</u>

Each binder ingredient was combined in air atmosphere at 177°C (350°F) and 15 psi (.103 MPa). The binder mixing was completed in 45 minutes, powder loading in 15 minutes, and the feedstock mixing in 45 minutes.

The feedstock was gradually cooled to room temperature and hand granulated.

### Prototype Test Mold

The injection mold for the prototyped test specimen was produced by Diversified Mold, Inc. (Huntington Beach, CA). Figure 5 shows a schematic illustration and a dimensional diagram with the "green" test bar dimensions (in metric units) before sintering. The shape of the die has some **degree of complexity** as the gauge section gradually narrows down from the wider areas, where the specimen is usually gripped during tensile testing. This shape demonstrated the capability of the **feedstocks** to be injection molded and provide a test specimen for determining the tensile properties.

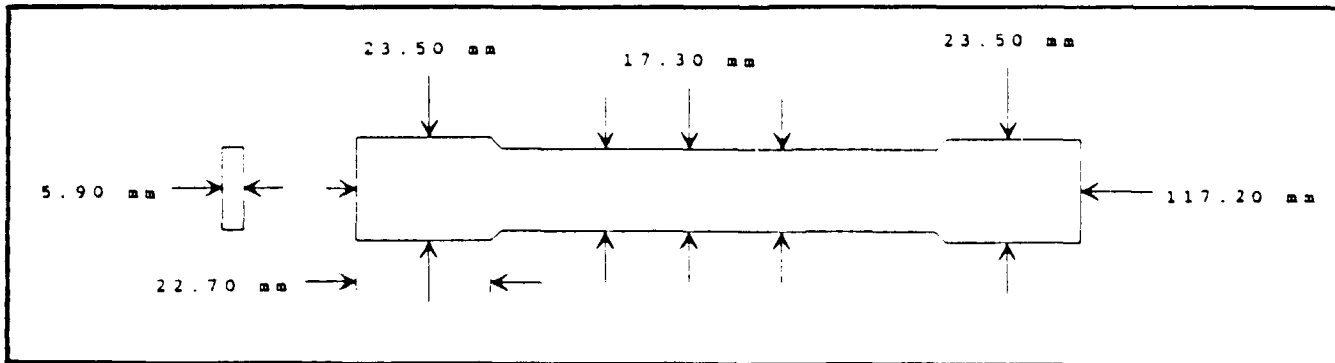
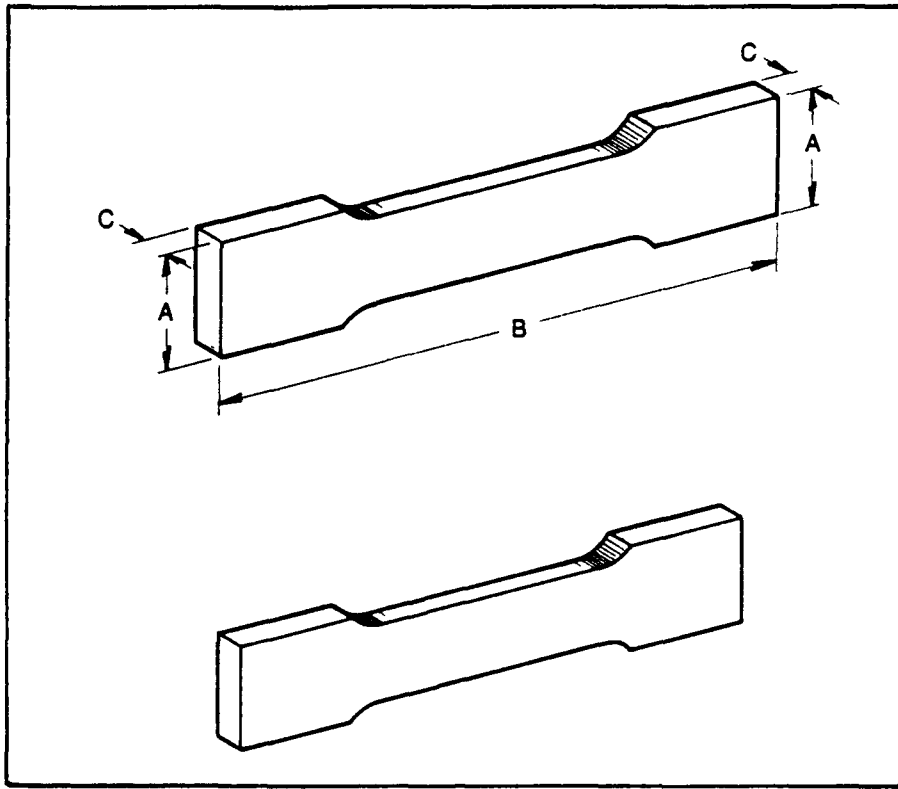


Figure 5. Illustration of Tensile Test Bar Specimen.

## Injection Molding

The prototype test specimens were created in a Arburg Injection Molding machine (Model 305-211-700). The molding conditions were:

Temperature:	Nozzle - 177°C (350°F)
	Front - 177°C (350°F)
	Middle - 177°C (350°F)
	Rear - 171°C (340°F)
Time Profile:	Injection - 6 sec.
	Hold - 2 sec.
	Cool - 18 sec.
Pressure:	Injection - 500 psi (3.445 MPa)
	Hold - 500 psi (3.445 MPa)

A total of 22 test bar specimens were molded. Nine were 0.50 volume loading and thirteen were 0.40 volume loading. The injection molded green bars were carefully weighed and their dimensions measured along the sections shown in Figure 5, marked "A" (width), "B" (length), and "C" (thickness). Two widths, one length, and two thicknesses were measured for each green tensile bar to determine the uniformity of shrinkage after sintering. Inappropriate injection molding conditions can create the possibility of obtaining flow induced non-uniformity, which would be displayed in the shrinkage results.

## Debinding (Solvent)

A combination of solvent and thermal debinding was utilized for two reasons: 1) Thermal binder extraction is very slow and can create excess gas pressure within green parts resulting in severe cracking and distortion, and 2) Thermal debinding can leave binder residuals which induce carbon content in the sintered microstructure.

The TAC process sequentially extracts portions of the binders leaving enough to provide adequate debound part strength. The test bars were chemically debound for eight hours in 1-1-1 trichloroethane and dried for twelve hours using a hot air circulator in a Bowden Liquid Turbo Charged system.

Furnacing (Thermal Debinding and Sintering)

Eighteen (18) solvent debound test specimens were sent to GTE Products Corporation (Towanda, PA) and were sintered under the supervision of Dr. James Mullendore. **Four sets** of test samples were obtained:

- 1) L.L. Test Bars sintered at 1480°C (2,696°F).
- 2) L.L. Test Bars sintered at 1520°C (2,768°F).
- 3) H.L. Test Bars sintered at 1480°C (2,696°F).
- 4) H.L. Test Bars sintered at 1520°C (2,768°F).

All samples were processed according to the following **furnacing schedule** with sintering temperatures of 1480°C (2,696°F) and 1520°C (2,768°F):

<u>Stage</u>	<u>Beginning Temperature</u>	<u>Ending Temperature</u>	<u>Ramp Rate Per Minute</u>	<u>Atmosphere</u>
Debinding (1)	Room Temp.	400°C (752°F)	2.2°C (4°F)	Dry H <sub>2</sub>
" (2)	400°C (752°F)	600°C (1112°F)	.33°C (.6°F)	Dry H <sub>2</sub>
" (3)	600°C (1112°F)	Room Temp.	5°C (9°F)	Dry H <sub>2</sub>
Presinter 1 (1)	Room Temp.	1200°C (2192°F)	10°C (18°F)	Dry H <sub>2</sub>
" (2)	1200°C (2192°F)	1200°C (2192°F)	Constant - 3 hrs.	Dry H <sub>2</sub>
" (3)	1200°C (2192°F)	Room Temp.	Furnace Cool	Dry H <sub>2</sub>
Presinter 2 (1)	Room Temp.	1400°C (2552°F)	10°C (18°F)	Dry H <sub>2</sub>
" (2)	1400°C (2552°F)	1400°C (2552°F)	Constant - 3 hrs.	Dry H <sub>2</sub>
" (3)	1400°C (2552°F)	Room Temp.	Furnace Cool	Dry H <sub>2</sub>
Sintering	Room Temp.	Sintering Temps.	50°C (90°F)	Wet H <sub>2</sub>
	Sintering Temps.	Sintering Temps.	Constant- 45 min.	Wet H <sub>2</sub>
	Sintering Temps.	Room Temp.	30°C (54°F)	Wet H <sub>2</sub>
Heat Treatment	Room Temp.	1200°C (2192°F)	25°C (45°F)	Vacuum
	1200°C (2192°F)	1200°C (2192°F)	Constant- 3 hrs.	Vacuum
	1200°C (2192°F)	Room Temp.	Furnace Cool	Vacuum

Liquid phase sintering was completed in a wet hydrogen atmosphere to prevent *insitu* water vapor formation. The samples were heated and held three hours in a vacuum atmosphere to remove **hydrogen embrittlement** effects. The sintered samples were **lapped and polished** to facilitate hardness and tensile testing; and were returned to Southwest Research Institute and the U.S. Army for testing.

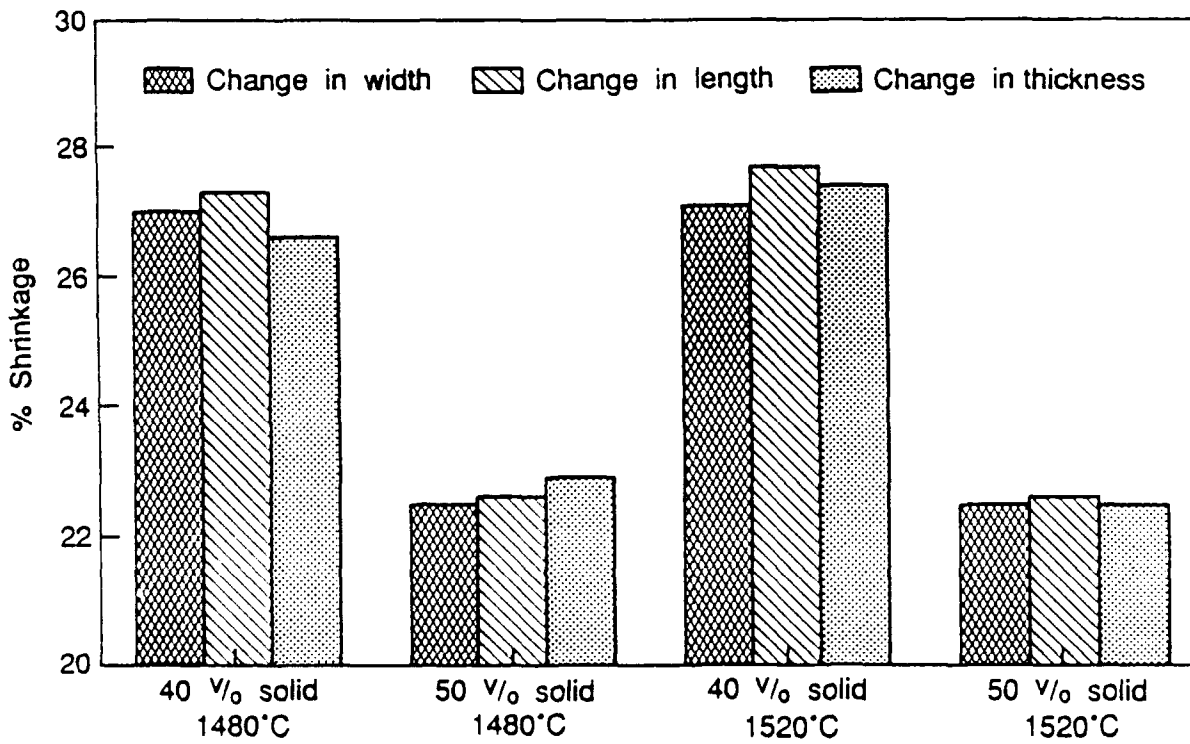
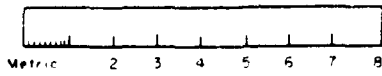


Figure 6. Test Bar Shrinkages.

## Part Dimensioning

The dimensions of all samples were measured to determine shrinkage. The shrinkages along the length, width, and thickness of the samples have been plotted in Figure 6. A photograph is also included to illustrate the difference in overall shrinkage for the H.L. (50% powder) and the L.L. (40% powder) samples. It can be observed that the variation in shrinkage between the three directions are within 1%. The actual variation in either width (A), length (B), or thickness (C), for each sample set is also less than 1%.

## Material Property Testing

The sintered density of the samples was measured using the water immersion technique with results summarized in Figure 7. All samples had a sintered density greater than 99.6% of theoretical. It is concluded that the PIM of heavy alloys resulted in near fully dense materials with negligible retained porosity.

The hardness of each sample was measured on the flat grip section to preserve the gauge section. At least twelve hardness indentations were taken, and the averages varied between 49.9 - 50.3 HRA. Microhardness measurements with a diamond indent were made on the tungsten grains and the matrix phase in the Vickers scale. The applied load for measuring the microhardness of the tungsten grains was 100 gm. and 10 gm. for the softer matrix phase. An average of four indentations was used to determine the Diamond Pyramid Hardness of the tungsten grains, while only two were used for the matrix phase. The microhardness averages are displayed in Figure 8.

The tensile properties of the samples were tested in an Instron with a crosshead speed of 0.05 inch/min. The yield strength (YS), ultimate tensile strength (UTS), percent elongation, and percent reduction in area of all the specimens are summarized in Figure 9. The yield strength and ultimate tensile strength of the material does not show any significant variation between the four sample sets investigated. The elongation values for the four different specimen sets ranged between 17 and 21%, with the L.L. samples showing slightly higher elongations. The higher solid volume fraction feedstock (0.5) was much more viscous and could result in small defects, which in turn would reflect on the elongation properties of the alloy.

The key result of Phase I was to determine if the tensile properties of the alloys processed by PIM displayed properties comparable to a similar alloy processed by press/sinter. The YS obtained in all four sets varied from 91.1 to 92.6 psi (628 to 638 MPa), the UTS 136.7 to 138.6 psi (942 to 955 MPa), and the elongation from 17 to 21%. These results were equal to results reported in the literature for 95W alloys.



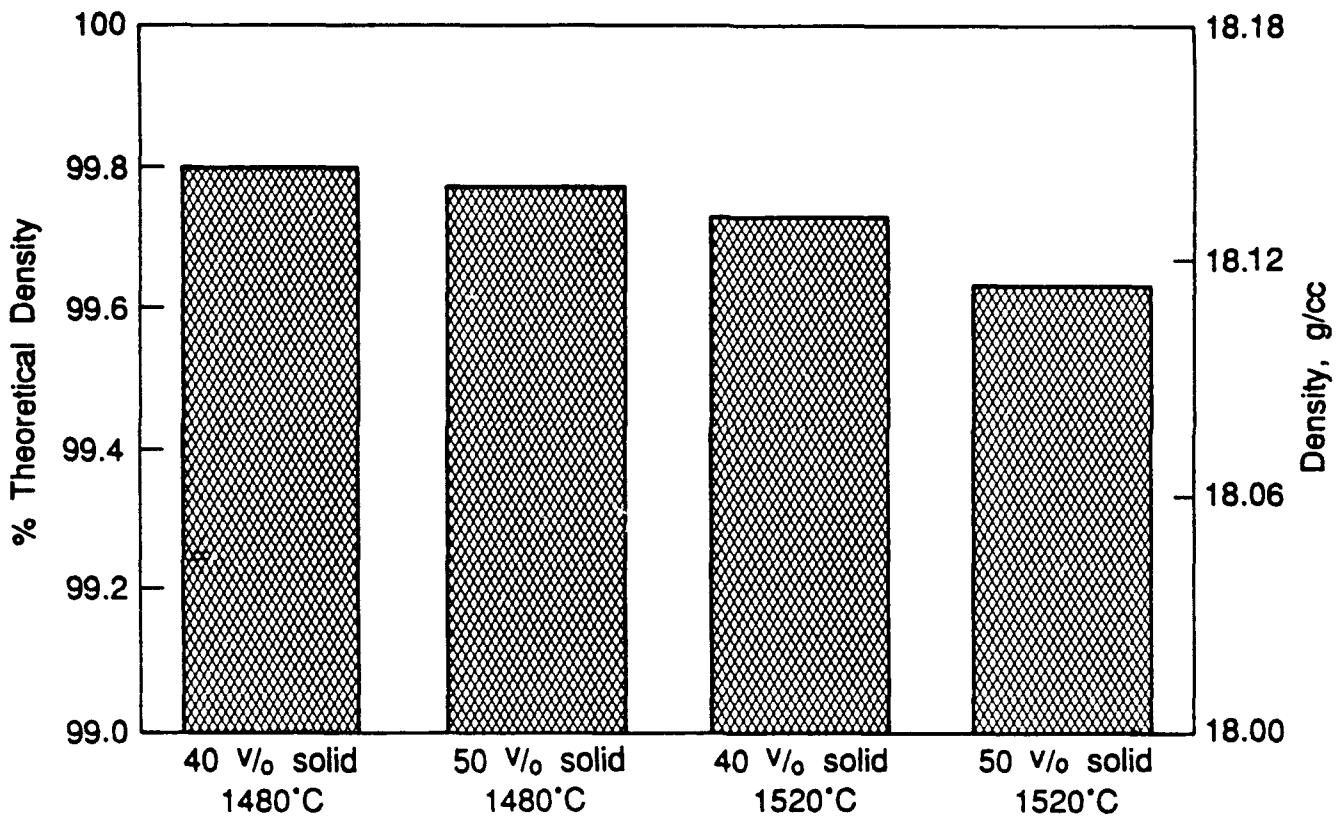


Figure 7. Test Bar Densities.

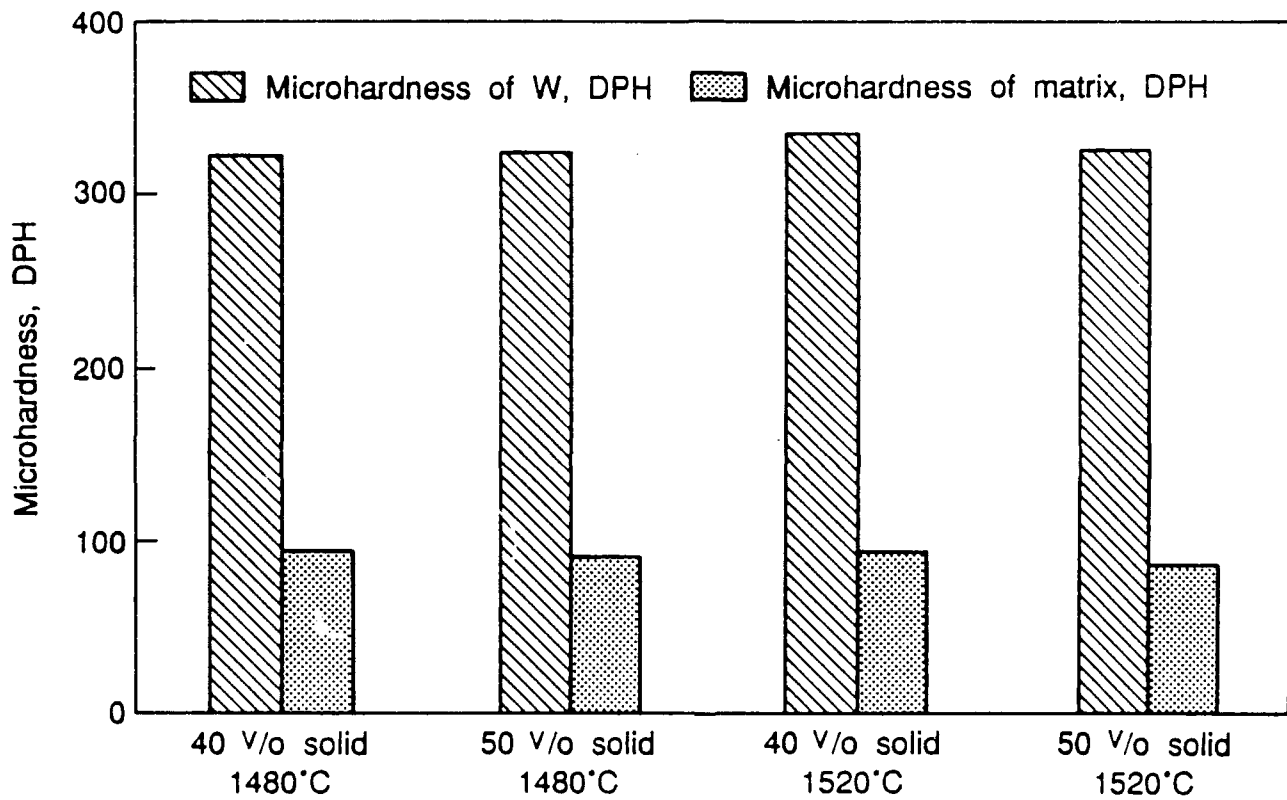


Figure 8. Test Bar Microhardness Data.

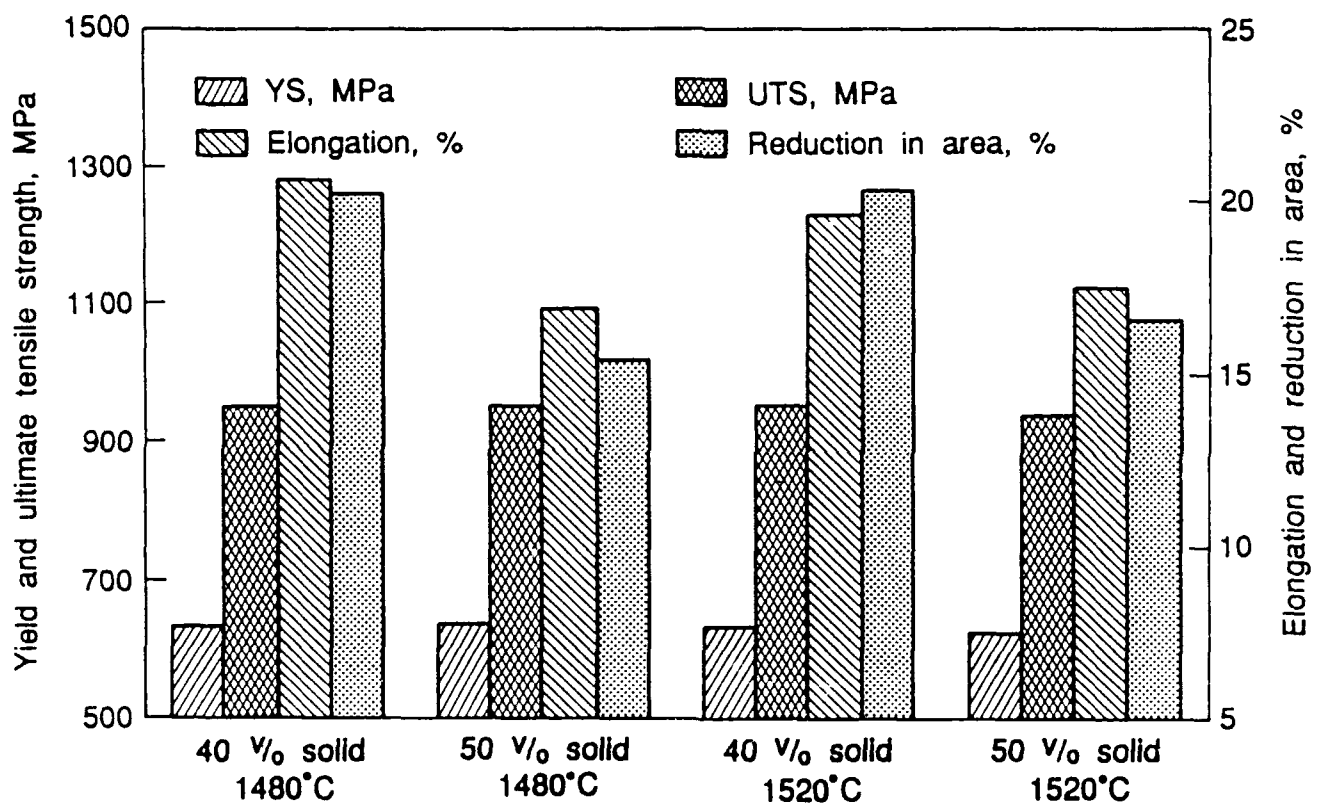
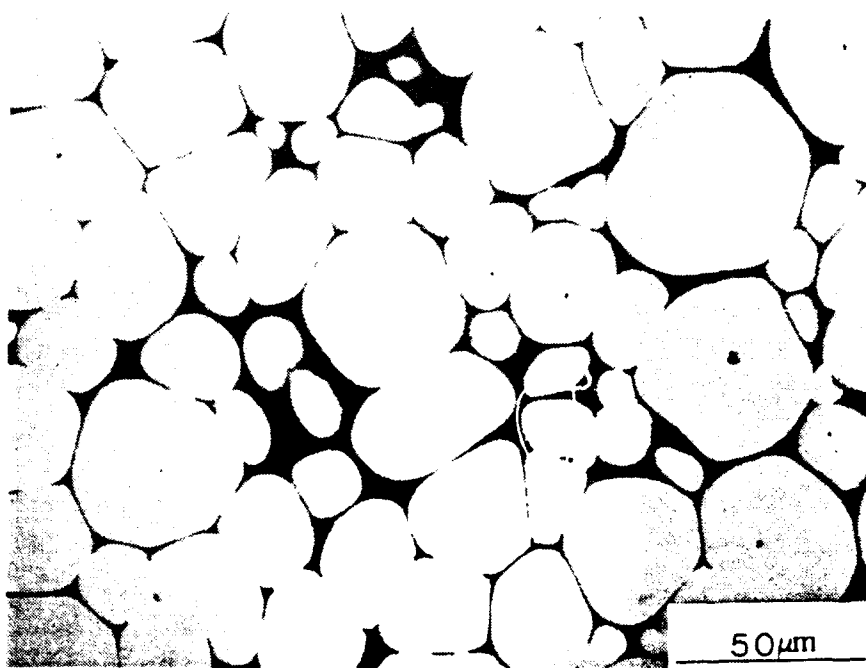


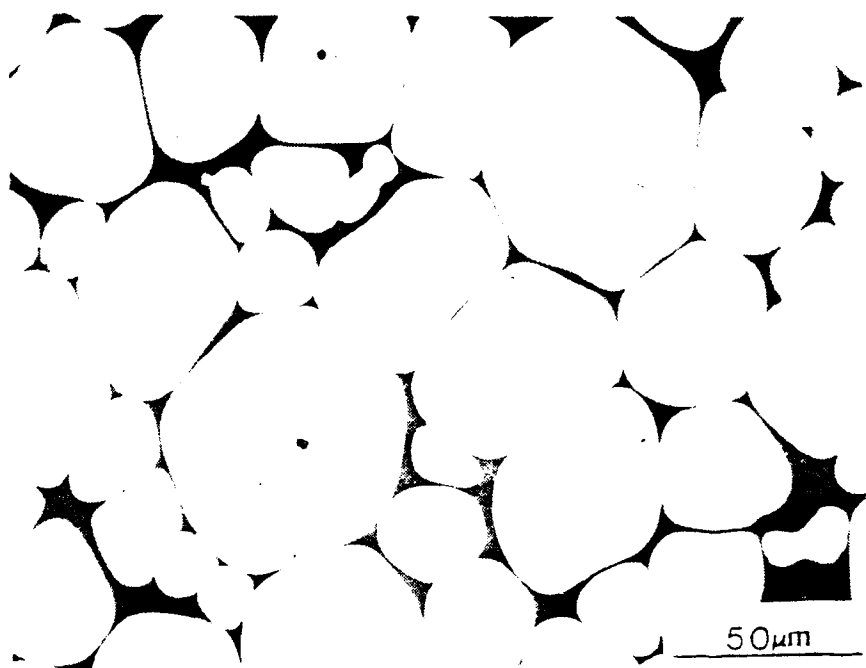
Figure 9. Test Bar Tensile Properties.

A microstructural characterization of the test samples was performed. Small sections removed from one end of a representative sample within each set were mounted, polished, and examined with a Scanning Electron Microscope (SEM). Microstructures were taken from selected areas, and a representative photomicrograph for the sample sets is shown in Figure 10 A and B. The microstructure displays spherical tungsten grains embedded in an alloy matrix of Ni, Fe and W. The microstructures had no porosity, except for the micro-pore that can be seen in the H.L. sample sintered at 1480°C.

The area fraction and the mean intercept length of the tungsten grains were measured from at least three areas with an automated image analyzer. The contiguous tungsten grains were manually dissected before measuring the mean intercept length of the tungsten grains. The results are shown in Figure 11 and are within the normal range of values exhibited by tungsten heavy alloys.

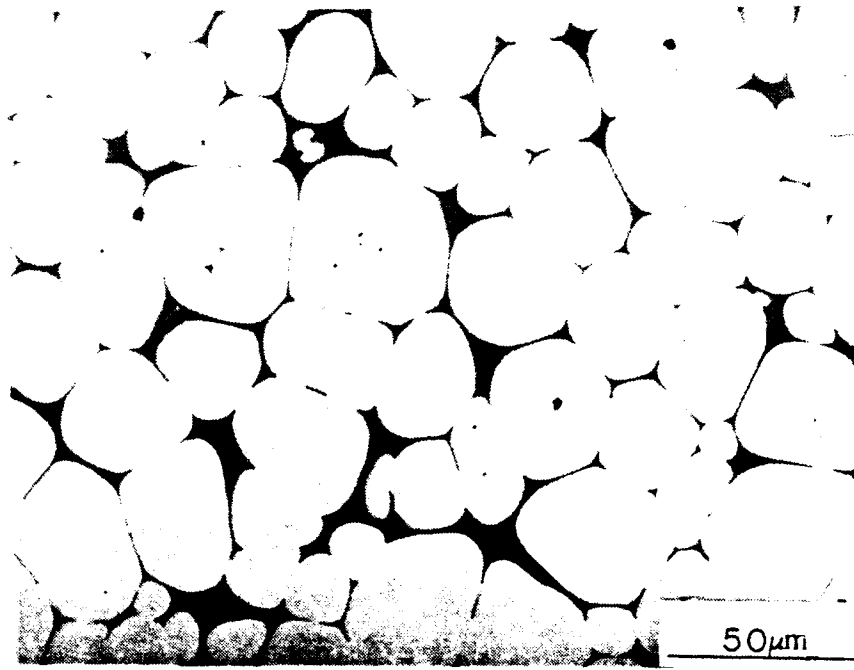


SEM photomicrograph of a heavy alloy sample with 0.4 volume fraction of solid, sintered at 1480°C.

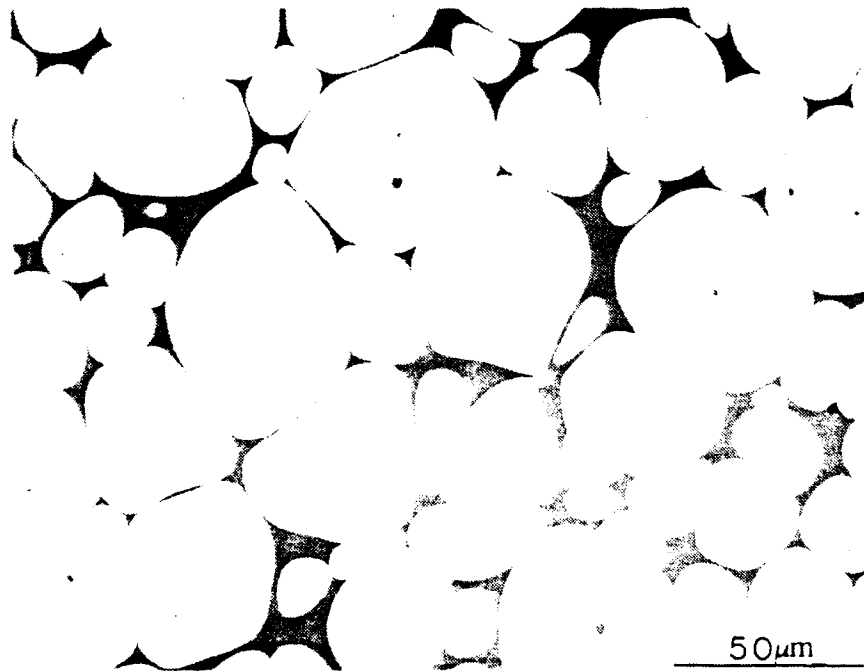


SEM photomicrograph of a heavy alloy sample with 0.4 volume fraction of solid, sintered at 1520°C.

Figure 10A. Microstructure SEM Photomicrographs.



SEM photomicrograph of a heavy alloy sample with 0.5 volume fraction of solid, sintered at 1480°C.



SEM photomicrograph of a heavy alloy sample with 0.5 Volume fraction of solid, sintered at 1520°C.

Figure 10B. Microstructure SEM Photomicrographs.

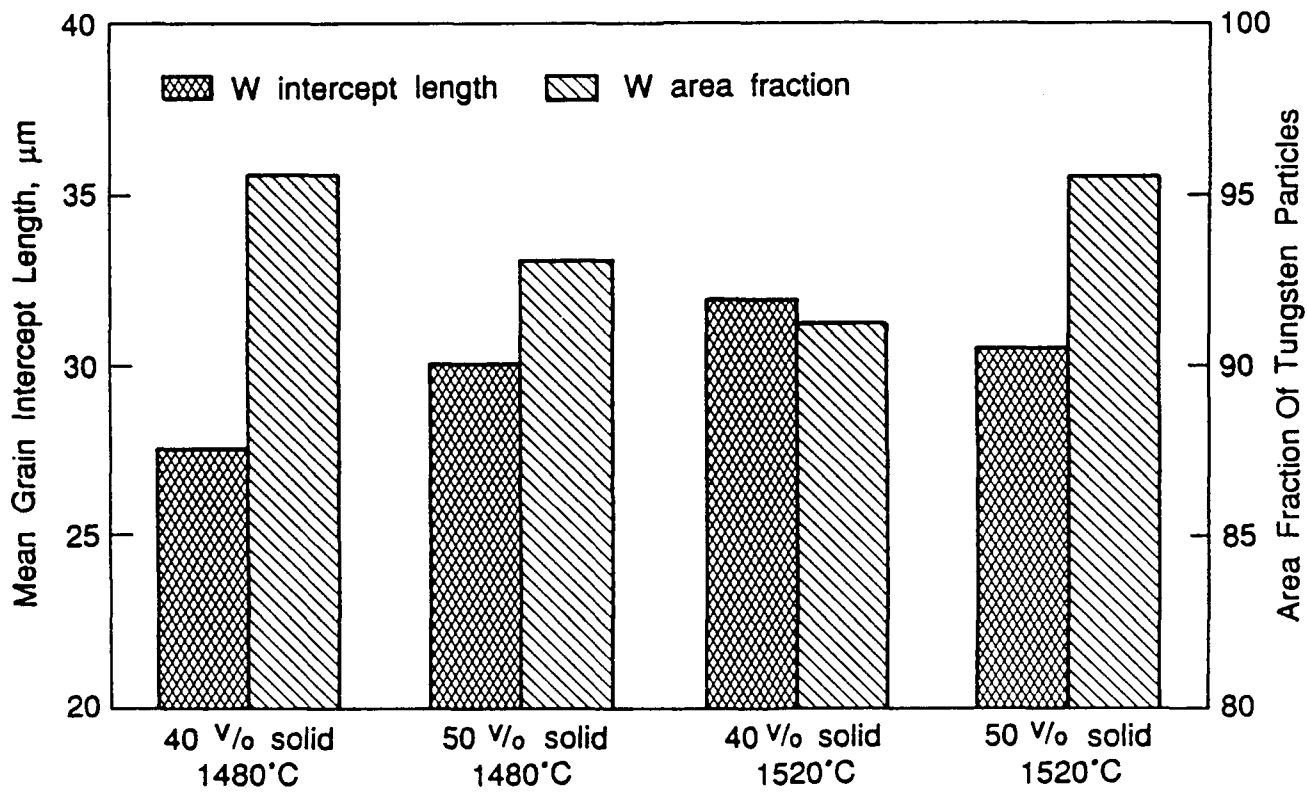


Figure 11. Tungsten Grain Characteristics.

## Chemical Analysis

The alloy chemistry of the matrix phase was evaluated by Energy Dispersive Spectroscopic (EDS) Analysis and is illustrated by the EDS spectra in Figures 12 A and B for the four sample sets.

Figure 13 shows the EDS spectra taken on a representative tungsten grain which reveals a pure tungsten content. The quantitative analysis of the matrix chemistry of all the samples showed the matrix alloy to have a composition of approximately 51Ni-38W-11Fe as illustrated in Figure 14.

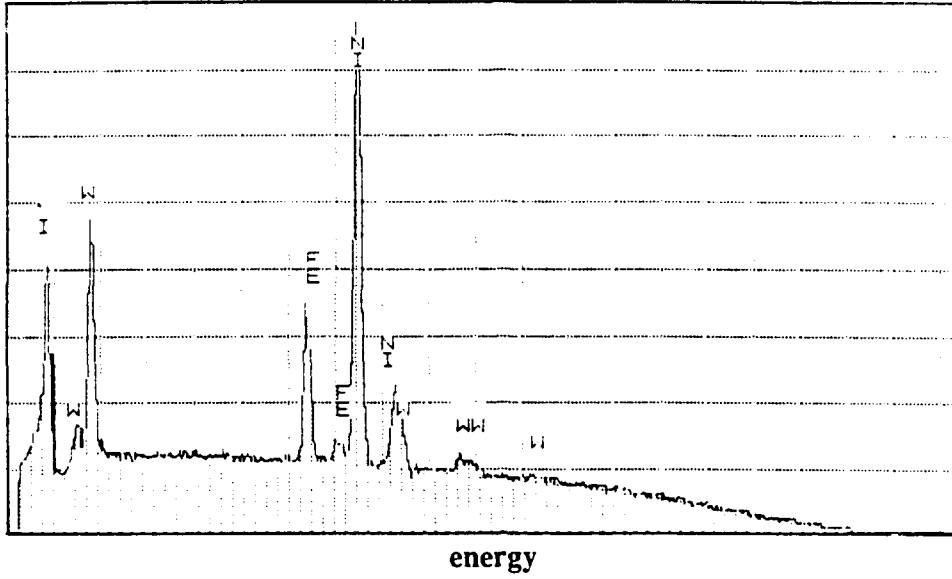
Carbon control in PIM of heavy alloys is a major concern since both carbon and oxygen can play a major role in decreasing resultant properties. The sintered PIM material and elemental powder blend were chemically analyzed by J. Dirats and Company (Westfield, MA) for both carbon and oxygen. The results indicated that the PIM processed materials did not result in any carbon or oxygen pick-up per the results presented in Figure 15. The notations included in this figure are summarized as follows:

<u>Notation</u>	<u>Meaning</u>
Sintered Part	Furnace Test Specimen
Powder S/N 1	Powdered Master Alloy - First Random Sample
Powder S/N 2	Powdered Master Alloy - Second Random Sample

During presintering and sintering, the reducing action of the hydrogen causes significant reduction in carbon and oxygen content due to the reactions that form water vapor, carbon dioxide, and carbon monoxide. This subsequently results in lower oxygen and carbon contents.

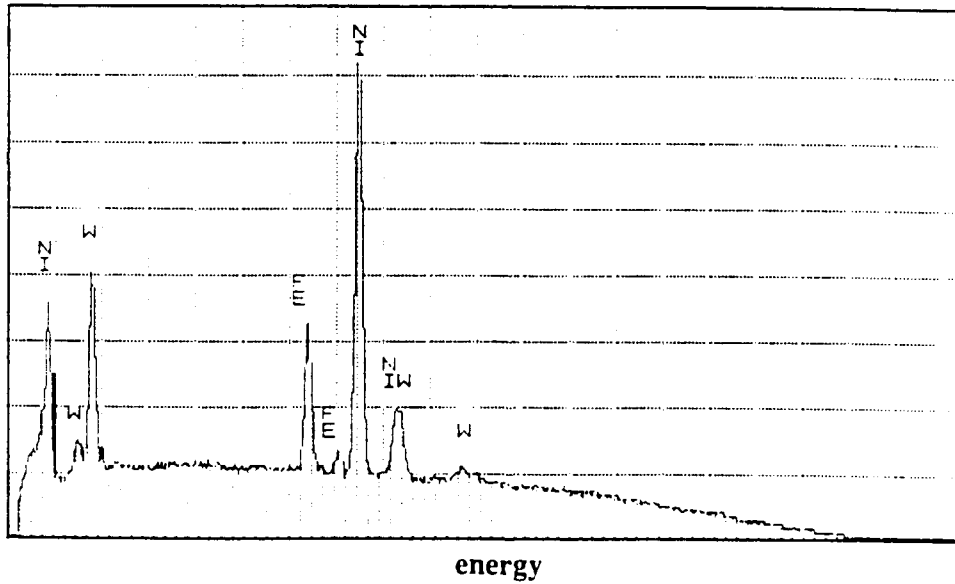


Relative  
Counts



EDS analysis of the matrix of a heavy alloy with 0.4 volume fraction of solid,  
sintered at 1480°C.

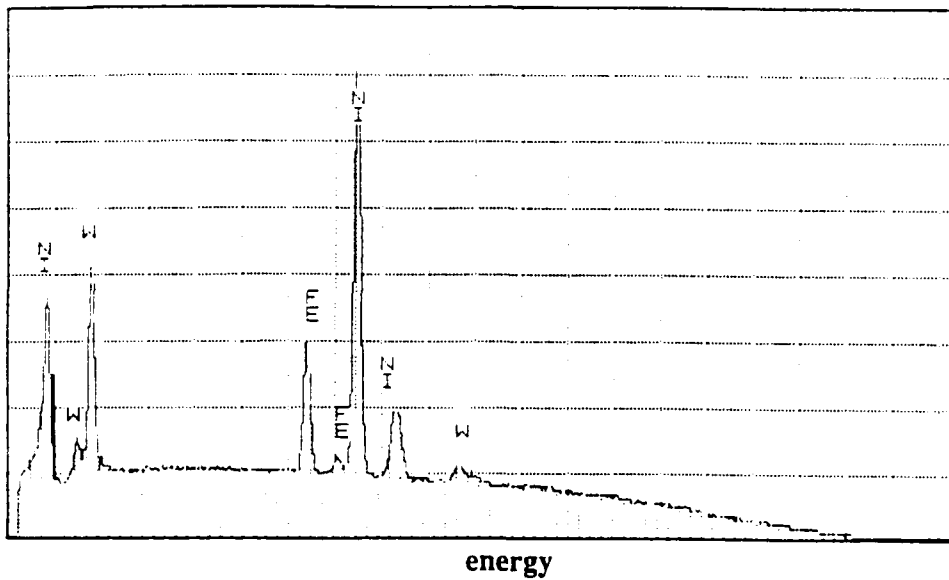
Relative  
Counts



EDS analysis of the matrix of a heavy alloy with 0.4 volume fraction of solid,  
sintered at 1520°C.

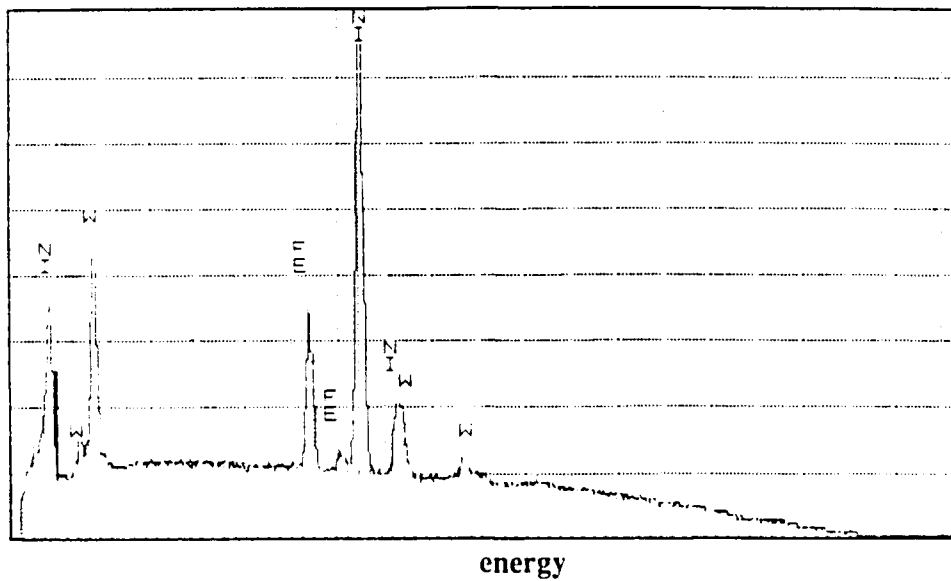
Figure 12A. Matrix Phase Alloy Chemistry.

Relative  
Counts



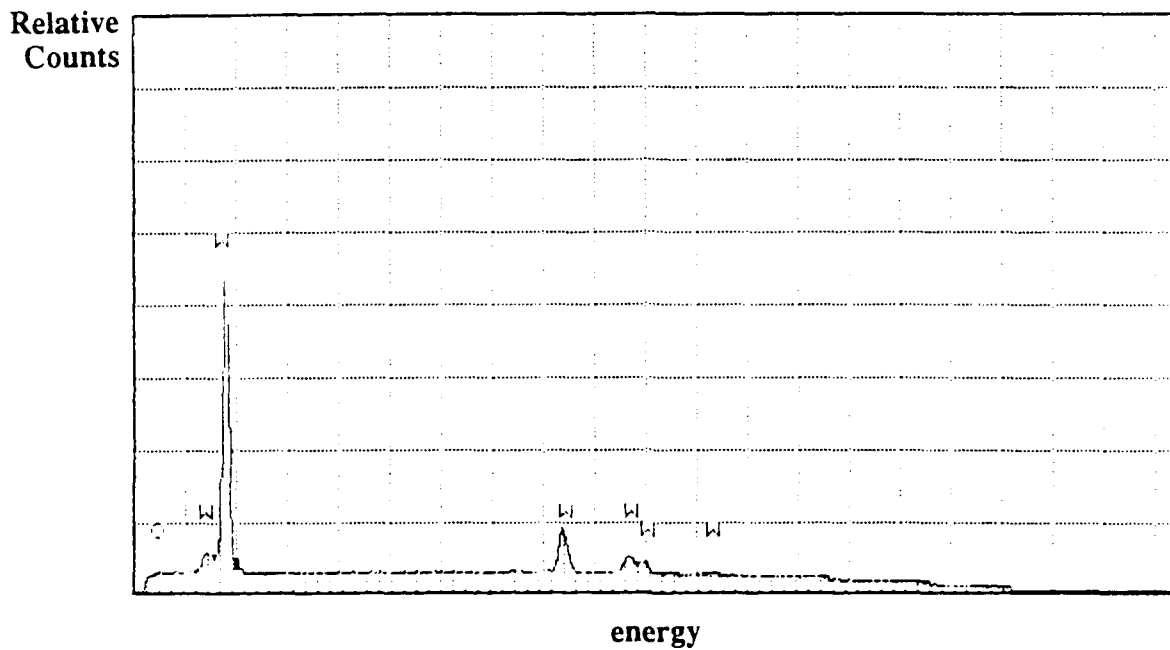
EDS analysis of the matrix of a heavy alloy with 0.5 volume fraction of solid,  
sintered at 1480°C.

Relative  
Counts



EDS analysis of the matrix of a heavy alloy with 0.5 volume fraction of solid,  
sintered at 1520°C.

Figure 12B. Matrix Phase Alloy Chemistry.



EDS analysis of a tungsten grain.

Figure 13. Tungsten Grain Alloy Chemistry.

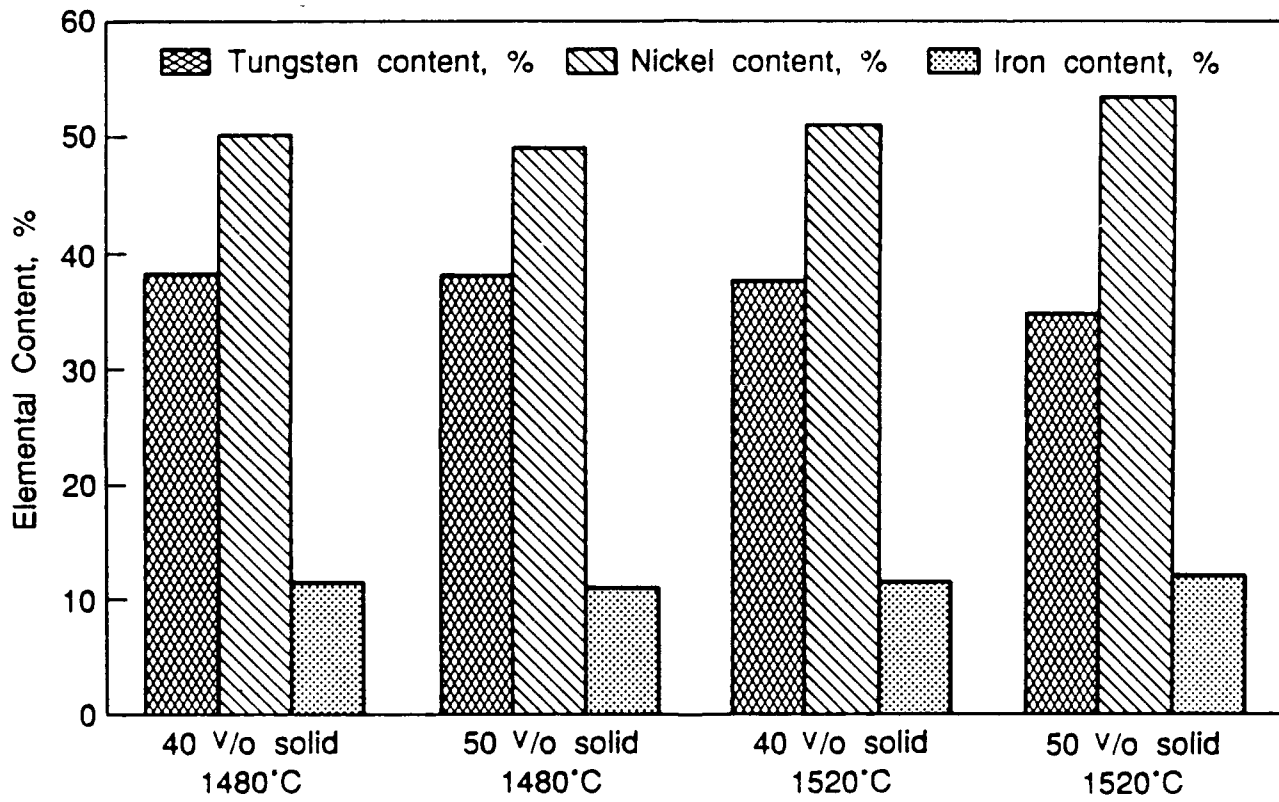


Figure 14. Matrix Chemistry - Quantitative Analysis.

Gary Allen  
 Technology Associates Corp.  
 17911 Sampson Lane  
 Huntington Beach, CA 92647

Report Number 139540  
 Report Date 7-MAY-91  
 Client Number \*\*816800  
 Client Order 2508

RECEIVED 1 Sintered Part and 2 Samples Powder  
 IDENT AS \*  
 MATERIAL W-Ni-Fe Alloy  
 CONDITION \*  
 TEST TO \*  
 TEST PER Client Instructions  
 PURPOSE \*

PHONE 714-842-8882

**PROPERTIES AS SUPPLIED**

**QUANTITATIVE ANALYSIS BY ICP, COMB.**

Sample %	SINTERED PART	POWDER S/N 1	POWDER S/N 2
W	95.19	94.66	94.71
Ni	3.75	4.01	3.98
Fe	0.99	1.03	1.03
N	0.0050	0.0301	0.0218
O	0.0073	0.2529	0.2465

Others:

Ti	0.02	<0.01	<0.01
Ta	0.02	<0.01	<0.01
Co	0.02	<0.01	<0.01
C	<0.01	0.01	0.01
S	0.002	0.004	0.005

For Info

For Info

For Info

The symbol < signifies not detected at the detectability limit indicated.

WE CERTIFY THIS IS A TRUE COPY OF OUR RECORDS

Signed for J. Dirats and Co. by Eric Dirats, Audit Manager

NOTE: The recording of false, fictitious or fraudulent statements or entries on this document may be punished as a felony under federal law.



Figure 15. Chemical Analysis.

## DISTRIBUTION LIST

No. of Copies	To
1	Office of the Secretary of Defense for Research and Engineering, The Pentagon, Washington, D.C. 20301 Commander, U.S. Army Laboratory Command, 2800 Powder Mill Road, Adelphi, MD 20783-1145
1	ATTN: AMSLC-IN-TL
1	ATTN: AMSLC-CT
2	Commander, Defense Technical Information Center, Cameron Station, Building 5, 5010 Duke Street, Alexandria, VA 22304-6145 DTIC-FDAC
1	MIAC/CINDAS, Purdue University, 2595 Yeager Road, West Lafayette, IN 47905 Commander, Army Research Office, P.O. Box 12211, Research Triangle Park, NC 27709-2211
1	ATTN: Information Processing Office
1	Dr. Andrew Crowson
	Dr. Edward Chen
1	Commander U.S. Army Materiel Command (AMC), 5001 Eisenhower Avenue, Alexandria, VA 22333 ATTN: AMCSOI
1	Commander, U.S. Army Materiel Systems Analysis Activity, Aberdeen Proving Ground, MD 21005 ATTN: AMXSY-MP, Director
1	Commander, U.S. Army Missile Command, Redstone Scientific Information Center, Redstone Arsenal, AL 35893-5241 ATTN: AMSMI-RD-CS-R/Doc
1	Commander, U.S. Army Armament Research Development and Engineering Center, Dover, NJ 07801 ATTN: Technical Library
1	Mr. D. Kapoor
1	Dr. S. Cytron
2	Commander, U.S. Army Tank-Automotive Command, Warren, MI 48090-5000 ATTN: AMSIA-TSL Technical Library
3	Commander, U.S. Army Foreign Science and Technology Center, 220 7th Street, N.E., Charlottesville, VA 22901 ATTN: AFETC, Applied Technologies Branch, Gerald Schleimer
1	Naval Research Laboratory, Washington, D.C. 20375 ATTN: Code 5830
1	Code 2627

No. of  
Copies

To

1 Chief of Naval Research, Arlington, VA 22217  
ATTN: Code 471

1 Air Force Armament Laboratory, Eglin Air Force Base, FL 32542  
ATTN: AFATL/DLYA, V.D. Thornton

1 Naval Surface Weapons Center, Dahlgren Laboratory, Dahlgren, VA 22416  
ATTN: Code G-32, Ammunition Branch, Mr. Brian Sabourin

1 Commander, Rock Island Arsenal, Rock Island, IL 61299-6000  
ATTN: SMCRI-SEM-T

1 Battelle Columbus Laboratories, Battelle Memorial Institute, 505 King  
Avenue, Columbus, OH 43201  
ATTN: Mr. Henry Cialone  
1 Mr. Robert Fiorentino

1 Battelle Pacific Northwest Laboratories, P.O. Box 999, Richland, WA 99352  
ATTN: Mr. William Gurwell  
1 Dr. Gordon Dudder

1 GIE Sylvania, Inc. Chemical and Metallurgical Division, Hayes Street,  
Towanda, PA 16848  
ATTN: Dr. James Mullenders  
1 Mr. James Spencer

1 Director, Ballistic Research Laboratory, Aberdeen Proving Ground, MD 21005  
ATTN: SPCBR-TSB-S (STINFO)  
1 SPCBR-TB-P, Mr. Lee Magness

1 Teconyne Earth Sterling, 1 Teledyne Place, LaVerne, TX 37086  
ATTN: Dr. Steven Caldwell  
1 Dr. Thomas Penrice

1 Technology Associates Corp., 17911 Sampson Lane, Huntington Beach, CA  
92647  
ATTN: Dr. Gary Allen

1 U.S. Army National Laboratory, ATAC, MS F684, P.O. Box 1063, Ft. Monmouth,  
NJ 08401  
ATTN: Dr. Louis Boron

1 United Fibers, 1000 Fishon Road, Lewiston, ME 04240  
ATTN: Mr. James Anderson

1 Cycronet, Inc., 12173 Montague Street, Pacoima, CA 91331  
ATTN: Dr. J.J. Stiglich  
1 Mr. Brian Williams  
1 Dr. Robert Tuffins

1 Genscon, Inc., 1101 N. Market Boulevard, Suite 9, Sacramento, CA 95811  
ATTN: Dr. Raj Raman

No. of  
Copies

To

Southwest Research Institute, 6220 Culebra Road, P.O. Drawer 28510, San Antonio, TX 78228-0510

1 ATTN: Dr. Animesh Bose  
1 Dr. James Lankford

Metalworking Technology, Inc., 1150 Scalp Avenue, Johnstown, PA 15904

1 ATTN: Mr. C. Buck Skena  
1 Mr. Timothy McCabe

Research Triangle Institute, P.O. Box 12194, Research Triangle Park, NC 27709-2154

1 ATTN: Dr. John K. Posthill

3C Systems, 620 Argyle Road, Wynnewood, PA 19096

1 ATTN: Mr. Murray Kornhauser

Advance Technology Coatings, 300 Blue Smoke Ct. West, Fort Worth, TX 76117

1 ATTN: Mr. Grady Sheek

Alliant Techsystems, 7225 Northland Drive, Brooklyn Park, MN 55428

1 ATTN: Dr. Stan Nelson  
1 Mr. Mark Jones  
1 Mr. Thomas Steigauf

CMBFC, 3002 Dow Avenue, Suite 110, Tustin, CA 92680

1 ATTN: Dr. Richard Darlow

Chamberlain Manufacturing Co., 550 Esther St., P.O. Box 2545, Watgrove, IA 50704

1 ATTN: Mr. Tom Lynch

Defense Technology International, Inc., The Starb. House, 22 Concord Street, Nashua, NH

1 ATTN: Mr. Douglas Ayer

Materials and Electrochemical Research Corporation, 700 S. 14th Road, Tucson, AZ 85706

1 ATTN: Dr. James Withers  
1 Dr. Smart Gohs

Materials Modification, Inc., P.O. Box 1517, Edinboro, PA 16710

1 ATTN: Dr. J.S. Sridharan

Micro-Materials Technology, 120 Research Drive, Millard, CT 06457

1 ATTN: Dr. Richard Cheney

Nuclear Metals, 2120 North Street, Concord, NC 27012

1 ATTN: Dr. William T. Hladky

Olin Industries, 1401 24th Street N., St. Petersburg, FL

1 ATTN: Bruce McFarlane



---

No. of  
Copies

To

---

The Pennsylvania State University, Department of Engineering Science and  
Mechanics, 227 Hammond Building, University Park, PA 16802-1401

1 ATTN: Dr. Randall M. German, Professor, Brush Chair in Materials

Director, U.S. Army Materials Technology Laboratory, Watertown, MA 02172-  
0001

2 ATTN: SLCMT-TML

1 SLCMT-IMA-V

1 SLCMT-PRC

27 SLCMT-MEM, Mr. Robert Dowding, COR

U.S. Army Materials Technology Laboratory  
Watertown, Massachusetts 02172-0001  
METAL INJECTION MOLDING OF TUNGSTEN  
HEAVY ALLOYS: SBIR PHASE I  
Gary M. Allen  
Technology Associates Corporation  
17911 Sampson Lane  
Huntington Beach, CA 92647  
Technical Report TR 91-37, October 1991, 34 pp -  
illus., Contract DAAL04-90-C-0018  
Final Report - 8/20/90 - 6/20/91

AD

UNCLASSIFIED  
UNLIMITED DISTRIBUTION

Key Words

Tungsten alloys  
Injection molding  
Powder injection molding

The objective of SBIR A90-133 is to investigate the feasibility of injection molding tungsten heavy alloys into net or near-net shape parts. The focus of Phase I was to demonstrate (on a laboratory scale) that powder injection molding (PIM) can provide parts with equivalent or superior sintered material properties to those that have been achieved for press/sintering heavy alloys of similar compositions. In addition, geometric shrinkage(s) and key process variables were identified and analyzed.

U.S. Army Materials Technology Laboratory  
Watertown, Massachusetts 02172-0001  
METAL INJECTION MOLDING OF TUNGSTEN  
HEAVY ALLOYS: SBIR PHASE I  
Gary M. Allen  
Technology Associates Corporation  
17911 Sampson Lane  
Huntington Beach, CA 92647  
Technical Report TR 91-37, October 1991, 34 pp -  
illus., Contract DAAL04-90-C-0018  
Final Report - 8/20/90 - 6/20/91

AD

UNCLASSIFIED  
UNLIMITED DISTRIBUTION

Key Words

Tungsten alloys  
Injection molding  
Powder injection molding

The objective of SBIR A90-133 is to investigate the feasibility of injection molding tungsten heavy alloys into net or near-net shape parts. The focus of Phase I was to demonstrate (on a laboratory scale) that powder injection molding (PIM) can provide parts with equivalent or superior sintered material properties to those that have been achieved for press/sintering heavy alloys of similar compositions. In addition, geometric shrinkage(s) and key process variables were identified and analyzed.

U.S. Army Materials Technology Laboratory  
Watertown, Massachusetts 02172-0001  
METAL INJECTION MOLDING OF TUNGSTEN  
HEAVY ALLOYS: SBIR PHASE I  
Gary M. Allen  
Technology Associates Corporation  
17911 Sampson Lane  
Huntington Beach, CA 92647  
Technical Report TR 91-37, October 1991, 34 pp -  
illus., Contract DAAL04-90-C-0018  
Final Report - 8/20/90 - 6/20/91

AD

UNCLASSIFIED  
UNLIMITED DISTRIBUTION

Key Words

Tungsten alloys  
Injection molding  
Powder injection molding

The objective of SBIR A90-133 is to investigate the feasibility of injection molding tungsten heavy alloys into net or near-net shape parts. The focus of Phase I was to demonstrate (on a laboratory scale) that powder injection molding (PIM) can provide parts with equivalent or superior sintered material properties to those that have been achieved for press/sintering heavy alloys of similar compositions. In addition, geometric shrinkage(s) and key process variables were identified and analyzed.

U.S. Army Materials Technology Laboratory  
Watertown, Massachusetts 02172-0001  
METAL INJECTION MOLDING OF TUNGSTEN  
HEAVY ALLOYS: SBIR PHASE I  
Gary M. Allen  
Technology Associates Corporation  
17911 Sampson Lane  
Huntington Beach, CA 92647  
Technical Report TR 91-37, October 1991, 34 pp -  
illus., Contract DAAL04-90-C-0018  
Final Report - 8/20/90 - 6/20/91

AD

UNCLASSIFIED  
UNLIMITED DISTRIBUTION

Key Words

Tungsten alloys  
Injection molding  
Powder injection molding

The objective of SBIR A90-133 is to investigate the feasibility of injection molding tungsten heavy alloys into net or near-net shape parts. The focus of Phase I was to demonstrate (on a laboratory scale) that powder injection molding (PIM) can provide parts with equivalent or superior sintered material properties to those that have been achieved for press/sintering heavy alloys of similar compositions. In addition, geometric shrinkage(s) and key process variables were identified and analyzed.